RERTR 2008 — 30th INTERNATIONAL MEETING ON REDUCED ENRICHMENT FOR RESEARCH AND TEST REACTORS

October 5-9, 2008
Hamilton Crowne Plaza Hotel
Washington, D.C. USA

CHARACTERISATION OF THE INTERACTION LAYER BETWEEN DECOMPOSED UMO7 AND ALUMINIUM USING MICRO-FOCUSED XRD ON A SINGLE PARTICLE

H. Palancher, E. Welcomme, C. Sabathier, P. Martin, F. Mazaudier, C. Valot, S. Dubois
CEA, DEN, DEC
F-13108 St Paul Lez Durance Cedex – France

R. Tucoulou
ESRF
6 rue Jules Horowitz, 38042 Grenoble - France

P. Lemoine
CEA, DEN, DSOE
F-91191 Gif-sur-Yvette Cedex – France

ABSTRACT

The interaction layer between decomposed γ-UMo7 and Al has been studied by annealing methods on atomized fuel plates. After a thermal treatment at 600°C during 10 hours, the growth of an interaction layer (IL) consisting of mainly UAl_3 and $U_6Mo_4Al_{43}$ but also of UAl_2 which has been seldom reported in the literature has been demonstrated. Moreover, the composition of the interaction layer appears heterogeneous and the UAl_2 concentration has been shown to increase from the outer to the inner part of the interaction layer. This work has been enabled by the power of the developed analytical technique (2D mapping using μ-XRD measurements) but also by the ability to study a single annealed UMo atomized particle extracted from fuel plates.
The interaction layer composition obtained by thermal annealing is very close to that of UMo10/Al samples irradiated in-pile at high temperature and up to a high burn-up confirming the predominant influence of the temperature parameter on the IL composition in these irradiation conditions.

1. Introduction

To fulfil non proliferation policy, the use of low ^{235}U enriched fuels (^{235}U weight concentration <20%) has to be strongly encouraged. This decision impacts mainly high performance research reactor cores which were working with highly enriched fuel (up to 93%). Common ceramic fuel materials do not allow such a reduction without any decrease of the core performances. For this reason researches are undertaken worldwide in the field of high density fissile materials. In this context, UMo/Al fuels are considered as the best candidates for LEU fuels.
However the behaviour under irradiation of these UMo/Al fuels is up to now not satisfactory because of the growth of a thick interaction layer (IL) at the UMo/Al interfaces [1,2,3]: the unacceptable fuel swelling, noted after in-pile irradiation, is attributed to the low fission gas retention capacities of this IL. Whatever the fuel design, UMo/Al interfaces are present either in the fissile part of the fuel (particle-matrix interface in the dispersion fuel concept) or at its periphery (cladding-fuel interface in the monolithic concept).
A breakthrough in the development of low ^{235}U enriched fuels has been performed recently with the first crystallographic characterisations of the IL appearing in in-pile irradiated

samples [4,5,6,7]. They pointed out the influence of the in-pile irradiation temperature on the nature (crystalline or amorphous) of the IL. Indeed TEM measurements have shown that the IL produced under low irradiation temperature, is amorphous [4], whereas this IL is crystalline in high temperature irradiated rods [5,6]. These conclusions have been confirmed by neutron diffraction experiments performed during the annealing of UMo/Al samples previously irradiated in-pile at low temperature: a transition from amorphous to crystalline phase has been observed [7].
However the precise composition of the interaction layer grown during in-pile irradiation at high temperature and up to a high burn-up (60%) remains difficult to interpret [6]. Although the temperature parameter seems to have played an important role in this irradiation test as shown by the decomposition of UMo7 gamma phase, this parameter does not seem to have had a predominant influence on the IL composition. Indeed neutron diffraction has shown the presence of the crystalline UAl_2 phase after in-pile irradiation although this phase has almost never been found in out-of-pile annealing experiments (it has only been reported once by diffraction [8]).
In the present work, further out-of-pile experiments have thus been performed using thermal annealing to investigate the presence or not of this UAl_2 phase in out-of –pile aged samples.
From a technical point of view, this work is based on innovative 2D mapping using µ-XRD measurements (X-ray diffraction using micro-focused beams) on a single particle selected and extracted from a pre-annealed UMo fuel plate. This analysis is based on the methodological advances performed when characterizing by µ-XRD thin UMo/Al fuel plate fragments [9].

2. Sample preparation and microscopy observations

Sample preparation, annealing and observations by microscopy have been performed at the “laboratoire Bernard François” facility of the Cadarache nuclear research centre.
γUMo7/Al fuel plates were provided by AREVA-CERCA[1]. Thermal annealing conditions were set to reproduce phenomena that had occurred during a Canadian in-pile irradiation [6]. Since γUMo cellular decomposition had been observed during the associated post-irradiation examinations, thermal annealing was also performed to decompose the γUMo7 phase. The precise conditions were: annealing at 600°C during 10 hours (under dry Ar/5%H_2 flux).
At a first step, the cladding was removed by successive mechanical polishing and the surface was prepared for observations. Laboratory examinations (optical and scanning electron microscopy) have revealed a thin (few micrometers) UMo/Al interaction layer surrounding UMo particles (cf. Figure 1).

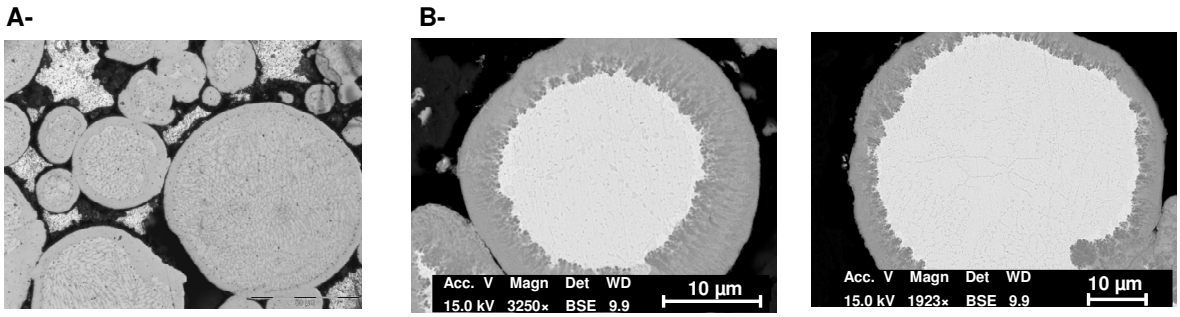

Figure 1: Observation of the UMo7/Al interaction layer grown in atomized particles after annealing at 600°C during 10 hours. Optical microscopy (A-) and SEM (back-scattered electrons) (B-).

Its thickness appears homogeneous in a first approximation. Interaction layer profile is close

[1] AREVA-CERCA, a subsidiary of AREVA-NP, an AREVA and Siemens company

to that reported in three previous annealing experiments carried out with UMo10 or UMo7 fissile atomized particles at temperatures ranging from 400°C to 600°C [8,10,11,12]. In this work, to precise SEM observations, EDX measurements were performed: they have demonstrated the heterogeneity of the IL, Mo element being more concentrated in the inner part than in the outer part.
At a second step, three atomized particles have then been isolated and each of them has been fixed on a glass capillary (cf. Figure 2) for µ-XRD measurements.
Optical micrograph shows that their diameter reaches about 50 µm.

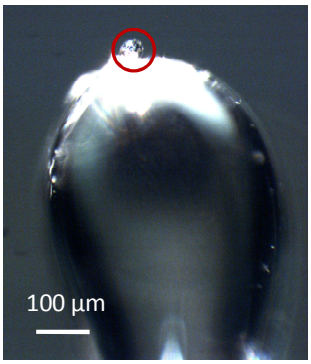

Figure 2: Optical micrograph of a single annealed particle fixed on a glass capillary

3. 2D mapping using micro-focused X-ray beams

XRD measurements using µ-focused X-ray beams have been carried on the ID18f beamline at the ESRF (Grenoble, France). This study is illustrated by the analysis of only one of the three particles, the characteristics of the two others being similar showing how representative is this particle.

3.a. Data collection

The energy of the X-ray beam was set to 28 keV and its size on the sample was 7×2µm². Diffraction data were collected in transmission mode using a MAR130 CCD camera (pixel size was about 78.5×78.5µm²). 2D mapping includes 713 images (31 lines per 23 rows). This mesh covers a 50×55µm² area.

3.b. Data treatment methodology

Before launching the automatic analysis of all collected diagrams, their summation has been performed for identifying the main crystallographic phases constituting this annealed particle.
For Rietveld refinement, the linux version of FullProf software package has been used [13]. Conversion of the XRD images to conventional 1D pattern was carried out thanks to the Fit2D software [14].

3.b.1 Analysis of an averaged diagram

At a first step all collected images were summed-up and the derived 1D pattern has been refined. Figure 3 shows both the average XRD image and the associated refined 1D pattern.

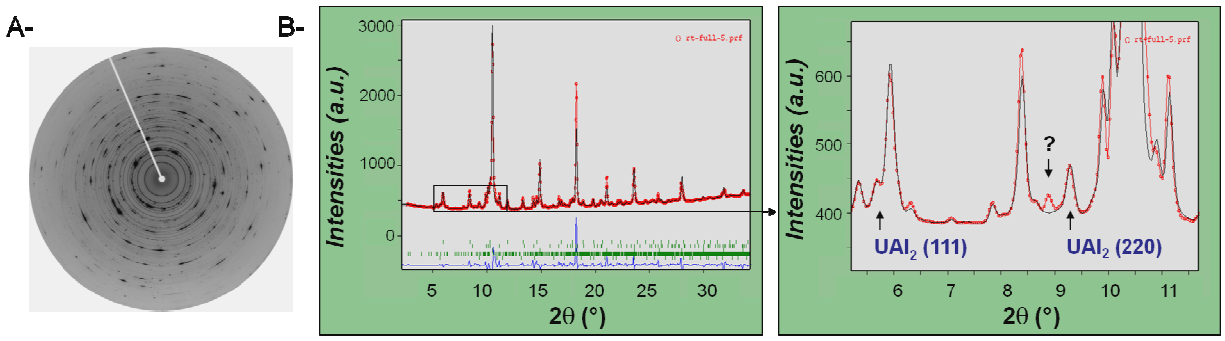

Figure 3: Summation of the µ-XRD images collected on the selected annealed particle (thermal treatment at 600°C during 10h). (A-) image and (B-) 1D associated refined pattern (left whole pattern, right magnified pattern.

The presence of five phases (αU, γUMo on the one hand and UAl_3, UAl_2, $U_6Mo_4Al_{43}$ on the other hand) has been evidenced. Decomposition rate of the gamma phase seems to remain limited (αU/(αU+γUMo7)≈20%) (cf. Table 1).

	UAl_3	αU	γUMo7	$U_6Mo_4Al_{43}$	UAl_2
UMo7/Al after annealing at 600°C during 10h	18.3±0.1	13±0.1	54.4±0.8	10.6±0.1	3.8±0.1
UMo7/Al after annealing at 600°C during 100h	74±2			26±2	

Table 1: Composition of the UMo7 particle previously annealed at 600°C during 10 hours. Figures are given in weight percent. As a comparison, another particle (annealed at the same temperature but a longer duration (100 hours) is also reported. More details on this study are given in the text (cf. §3.c.1.3).

The presence of the UAl_2 phase was the most difficult to identify. The concentration of this phase is rather low and peaks overlap with peaks of the UAl_3 and $U_6Mo_4Al_{43}$ phases which are higher. However two Bragg peaks ((111) and (220)) enable to unambiguously identify the UAl_2 phase.
Moreover, one extra peak remains unidentified (at 8.88°) and could not be indexed to an existing crystallographic phase (cf. Figure 3-B).

3.b.2 Analysis of the µ-XRD patterns

Data treatment methodology is based on automatic and independent refinement of each 1D pattern thanks to the Rietveld method [9]. At a first step, eight phases were considered: UAl_3, UAl_4, $U_6Mo_4Al_{43}$, γUMo7, U_2Mo, αU, UO_2 and UAl_2. In addition to the scale factor of these phases, four other parameters for background fitting were left free during the refinement. Confirming the analysis of the average 1D pattern, no significant concentration for UAl_4, U_2Mo and UO_2 phases has been found in this local analysis. In a last step only the five relevant crystallographic phases were taken into account.
Results of the automatic refinement have been post-treated to keep only most reliable values.
For binary and ternary compounds, three criteria have been determined for removing inaccurate refinement results (see below): when these criteria were not satisfied, weight concentrations were set to 0.

- the weight concentration has to be at least twice as high as the calculated error;
- a minimum value on the refined scale factor has been defined (3.10^{-7} for UAl_3);
- the agreement factor between calculated measured intensities for a given crystallographic phase (RBragg) has to remain lower than 35%.

For αU and γUMo only the two first criteria were used since RBragg values were generally quite high because of their high texture and poor sampling statistics.

3.c. Crystallographic composition of the particle

It has been possible to obtain the weight concentration maps associated to the five phases of interest. Figure 4 gathers these representations.
As shown on this figure, UAl_3, $U_6Mo_4Al_{43}$ and UAl_2 are located at the periphery of a core consisting of αU and $\gamma UMo7$. These conclusions are in good agreement with SEM observations (cf. Figure 1).

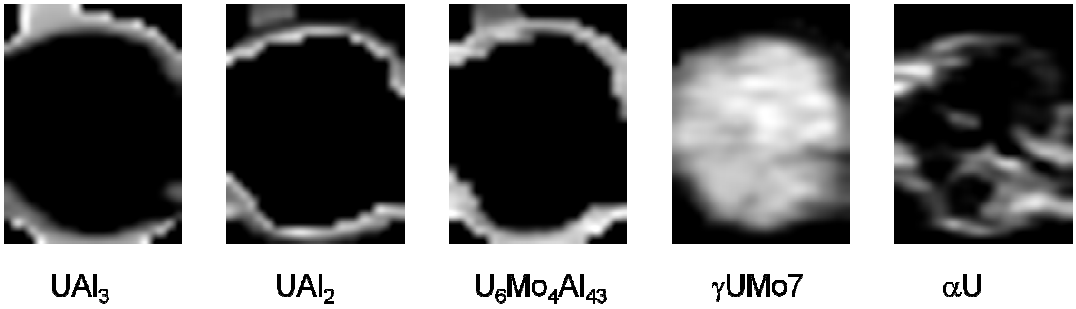

Figure 4: Weight concentration maps in a single UMo particle previously annealed at 600°C during 10 hours. (Colour code uses black to white for lowest to highest values).

3.c.1 interaction layer heterogeneity

In this work if the UMo/Al interaction has always been found to consist of three components, their relative concentrations are fluctuating inside the IL. In Figure 5, the proportion of each component of the IL (UAl_2, UAl_3 and $U_6Mo_4Al_{43}$) is shown. In this representation the weight concentration of each crystallographic phase has been divided by the summation of UAl_2, UAl_3 and $U_6Mo_4Al_{43}$ concentrations at each point of the 2D mapping.

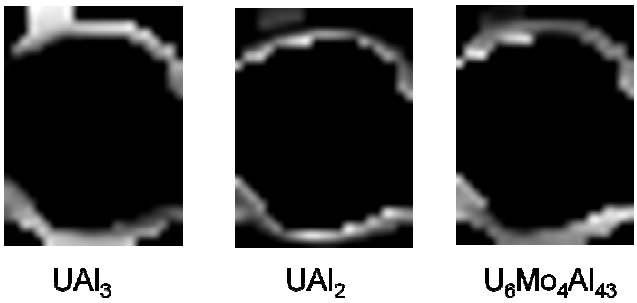

Figure 5: Normalized weight concentrations maps of each component of the interaction layer (UAl_2, UAl_3, $U_6Mo_4Al_{43}$) in a single UMo particle previously annealed at 600°C during 10 hours. (Colour code uses black to white for lowest to highest values).

3.c.1.1 Qualitative interpretation

A qualitative interpretation shows that the composition of the IL is heterogeneous. Indeed UAl_3 concentration is maximum in the outer part of the IL whereas UAl_2 concentration is higher at the interface between the IL and the UMo core. The $U_6Mo_4Al_{43}$ weight concentration is almost stable but increases slightly from the outer to the inner part of the IL.
In a first approximation it seems that $U_6Mo_4Al_{43}$ and the sum of UAl_3 and UAl_2 weight concentrations are constant in the thickness of the interaction layer.
This conclusion is illustrated by Figure 6: to stress the variations of weight concentration for each phase of the IL, a diagram has been preferred to maps

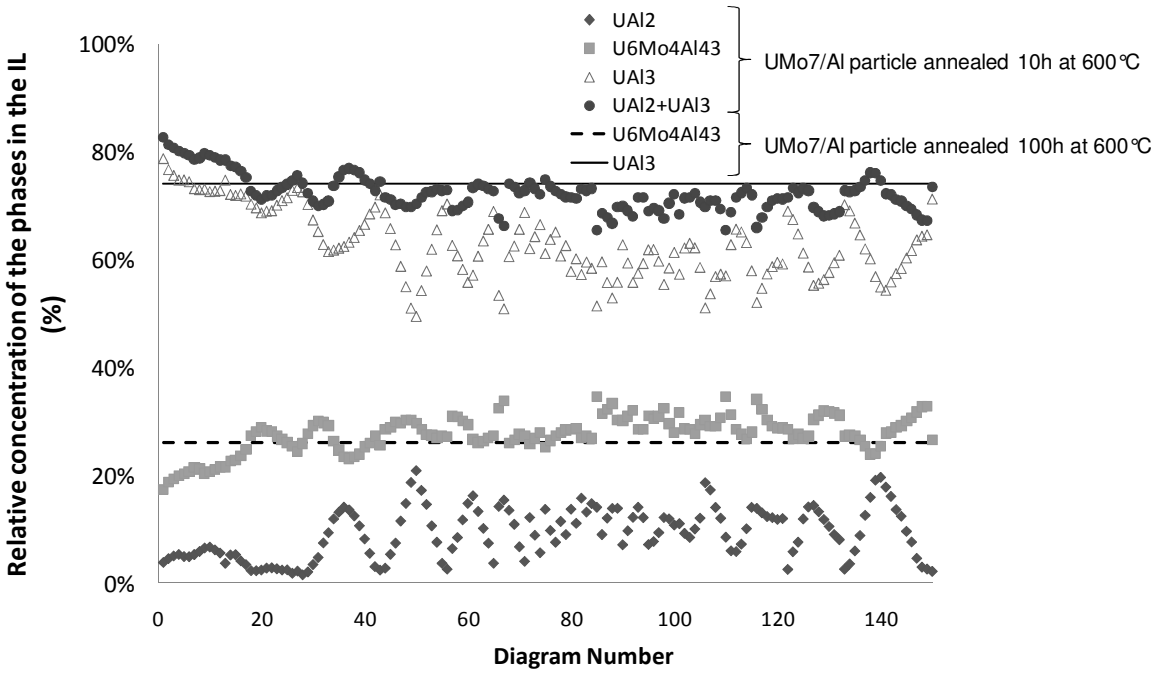

Figure 6: Composition of the interaction layer grown in the particle after a thermal treatment at 600°C during 10 hours. As a comparison, average composition of the interaction obtained on a particle annealed at 600°C during 100 hours is indicated on the figure (further details on this study are given in the text (cf. §3.c.1.3)).
In this graph, UAl_2, UAl_3, $U_6Mo_4Al_{43}$ weight concentrations are given only for a selection (150) of the 713 diagrams collected in the 2D mapping. Note that many diagrams have not been considered since they do not fulfil the post-treatment criteria of the Rietveld analysis i.e. weight concentrations have not been determined with enough accuracy (cf. § 3.b.2). This is especially the case when the proportion of these phases is too low in the characterized zone (particle core).
In this statistical representation, the number of the diagram is not directly linked to the probed volume of the sample. Only the fraction of each phase (ordinate) can be interpreted.

3.c.1.2 Semi-quantitative interpretation

A semi-quantitative interpretation shows that in the outer part of the IL, UAl_2, UAl_3 and $U_6Mo_4Al_{43}$ weight concentrations are 4±2, 69±5, 27±4% respectively but in the inner part, these concentrations fluctuate to become 14±2, 57±4, 29±3%. Differences between the compositions of the two sub layers are under estimated by this analytical technique. Indeed (2D mapping using µ-focused XRD) is not able to take into account sample heterogeneity in the depth: only an averaged value is provided (for further details, see §4).

3.c.1.3 UAl_3 and $U_6Mo_4Al_{43}$ weight concentrations analysis

To interpret more accurately the results of this semi-quantitative analysis and in particular the ratios between UAl_3 and $U_6Mo_4Al_{43}$ weight concentrations, the study of another kind of IL in which UAl_3 and $U_6Mo_4Al_{43}$ phases are only present has been decided. This second study will be used for a comparison.

The interaction between γUMo7 and Al has been chosen. With that aim, an UMo7/Al fuel plate has been annealed during 100 hours at 600°C. Optical micrograph, SEM images and interpretations have been given elsewhere [11], demonstrating that particles have been fully affected by the interaction with Al: no γUMo7 phase remained at the centre of the particle. The analytical methodology detailed in this communication for the sample annealed 10 hours at 600°C has also been applied on this sample: 2D mapping using micro-focused XRD has been performed on a unique particle selected after thermal treatment.

This particle has been found to be homogeneous in composition and only $U_6Mo_4Al_{43}$ and UAl_3 have been detected (cf. Figure 7). Note that contrary to X-ray diffraction measurements collected on the particle annealed 10 hours at 600°C, no shoulder is present at 5.69°(2θ) on the (100) UAl_3 peak, indicating the absence of the (111) reflection of the

UAl_2 phase (cf. Figure 3-B): it demonstrates the absence of this phase and confirms the interest of the technique for assessing or not its presence in the IL.
Rietveld analysis of these patterns leads to weight concentrations of 74±2 % and 26±2% for UAl_3 and $U_6Mo_4Al_{43}$ respectively. Since the same data collection geometry has been used for the measurements on particles annealed at 600°C during 10 and 100 hours, weight concentrations of UAl_3 and $U_6Mo_4Al_{43}$ can be quantitatively compared in both samples.

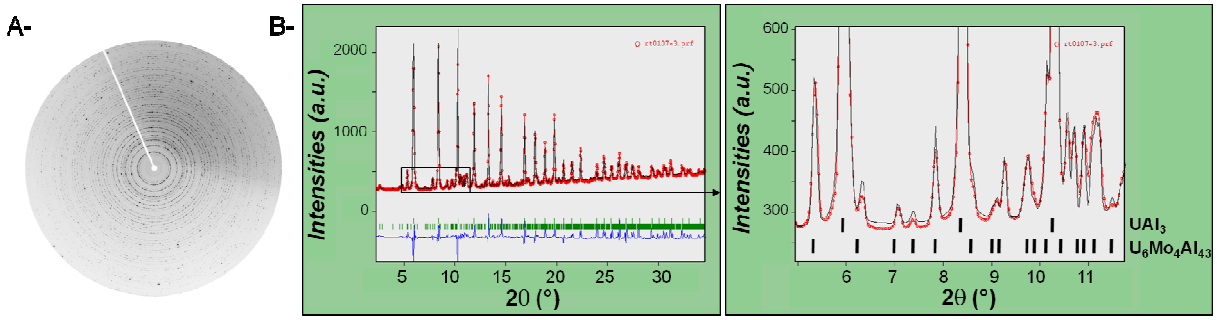

Figure 7: Example of µ-XRD image collected on the annealed particle (thermal treatment at 600°C during 100h). (A-) image and (B-) 1D associated refined pattern (left whole pattern, right magnified pattern).

It appears first that whatever the interaction process (γUMo7/Al or (γUMo7+αU)/Al), $U_6Mo_4Al_{43}$ has almost the same concentration in the two types of IL. This is clearly not the case for the UAl_3 phase: the sum of UAl_2 and UAl_3 weight concentrations in the sample annealed 10 hours is almost equivalent to the UAl_3 weight concentration in the sample annealed 100 hours (cf. Figure 6).

3.c.1.4 Mo location in the IL

Previous experiments have shown that Mo solubility in UAl_2 cannot be neglected contrary to UAl_3 or UAl_4 [9,15]. It has to be investigated whether Mo is only included in $U_6Mo_4Al_{43}$ or also in UAl_2. However considering the weight concentrations of UAl_2 and $U_6Mo_4Al_{43}$, it can be concluded from this work that the main part of Mo should be present in $U_6Mo_4Al_{43}$.
The clear increase of UAl_2 concentration and that more limited of $U_6Mo_4Al_{43}$ in the IL from the outer to the inner part of the IL has to be compared with EDX results which have pointed out a significant increase of the Mo content in the inner part. As an hypothesis, one can propose that in the inner shell of the IL, fraction of Mo located in UAl_2 is higher than in the outer shell.
To address definitely this issue, µ-EXAFS measurements would be necessary [9].

3.c.2 Characteristics of the annealed particle core after annealing during 10h at 600°C

As indicated by the U-Mo phase diagram [16], annealing of γUMo7 at 600°C has led to the decomposition of the gamma phase and to the formation of αU with no U_2Mo phase. Note also that the Mo enriched γUMo phase has not been detected. This result is in agreement with the low decomposition rate of the gamma phase shown in the average X-ray analysis (cf. § 3.b.1).

4. Discussion

4.a. Characterisation methodology

The interest of neutron diffraction and XRD in reflection mode for characterizing the cellular decomposition of the γUMo phase has been shown previously [8,17]. However these techniques suffer from a lack of spatial resolution which can be significantly improved by using µ-XRD in transmission mode. However, one main drawback of this last method is the limited X-ray penetration depth (1/e) in the very dense UMo crystallographic phase (about 11 µm at 28 keV); the penetration depth is higher in binary UAl_x or ternary $U_xMo_yAl_z$

compounds (more than 30 µm at 28 keV). For this reason, selected particles have to remain small (lower than 50 µm in diameter).
Moreover, since the diffracting volume is limited, sampling may be unsatisfactory if the crystallites size is too large. This is the case for the characterisation of γUMo or αU phases which seem to have large crystallite size which limit statistics and disturb X-ray diffraction peak intensity. In such case any quantitative analysis can be done, only the presence/absence of both phases may be discussed. However when probing the UMo/Al interaction layer this effect can be neglected since UAl_3, $U_6Mo_4Al_{43}$ and UAl_2 exhibit low sized crystallites (the diffracted intensity is homogeneously distributed around Debye Scherrer ring associated with those phases (cf. Figure 3-A). A semi-quantitative analysis of the diagrams can be performed and weight concentration of each phases derived.
As discussed elsewhere [18], X-ray diffraction computed tomography using nano X-ray beams may lead to a full 3D reconstruction of crystallographic composition. However when analysing samples with a known and simple geometry (spherical particles with a homogeneous interaction layer surrounding the unaffected core), 2D mapping using µ-XRD is a powerful technique to analyse the composition of the IL.

4.b. Occurrence of the UAl_2 phase in the IL produced by thermal annealing

Two works reported in literature proposed the presence of the UAl_2 phase in the IL between decomposed γUMo7 and Al, one on the basis of EPMA analyses [19], the other on the basis of diffraction data [8]. In this last case, (U_2Mo+αU)/Al interaction has occurred: the authors have suggested that the presence of UAl_2 phase in the IL is connected with the appearance of U_2Mo phase.
The results of the present work seem to contradict this interpretation since UAl_2 has been found in a sample which does not include any U_2Mo. However the presence of this UAl_2 phase is systematically associated to the reaction of Al with the decomposed γUMo phase. In this work, the additional presence of $U_6Mo_4Al_{43}$ has been proven.
However it must be stressed that all annealing experiments performed for studying the interaction between decomposed γUMo7 and Al that have been reported in the literature did not evidence the formation of the UAl_2 phase. Moreover, in many cases, these last experiments have been carried out at temperatures very close to those chosen for this work (600°C) [20]. This question has to be further investigated.

4.c. Interpretation of the IL composition grown in-pile at high burn-up and under high temperature

Recent neutron powder experiment enabled to show that the IL grown in UMo10/Al after in-pile irradiation up to 60% burn-up, consists of 79wt%UAl_3, 20wt% UAl_2 and 1wt % UMo_2Al_{20} [6]. This composition appears very similar to that obtained in this study on a thermal annealed sample: the binary phases identified are the same. It clearly shows that during this irradiation the temperature has played a predominant role on the composition of the IL.
However no $U_6Mo_4Al_{43}$ has been found in the in-pile irradiated fuel whereas the amount of this phase is low but significant in the out-of pile thermally treated one. Two explanations can be proposed. First of all, interaction types are not strictly equivalent since in the first case (in pile [6]), decomposition of the gamma phase leads to the formation of U_2Mo+αU while in the second case (this study) γUMo + αU have been identified. Secondly, irradiation effects may explain part of this difference (absence of $U_6Mo_4Al_{43}$) because they can lead to phase transition or amorphisation.

5. Conclusion

The interaction between decomposed UMo (γUMo + αU) on the one hand and Al on the other hand has been studied in details by 2D mapping using µ-XRD of an isolated pre-annealed particle. This study has revealed the presence of three main phases in the interaction layer: UAl_3, $U_6Mo_4Al_{43}$ and UAl_2. Their individual relative proportions have been

found to fluctuate inside the IL (UAl_3 weight concentration being maximal in the outer part contrary to UAl_2) while the weight concentrations of UAl_2 +UAl_3 on one hand and $U_6Mo_4Al_{43}$ on the other hand have been found to be almost constant in a first approximation whatever the location inside the IL.

This study has demonstrated that the crystalline UAl_2 phase can be grown by thermal annealing and such a result is of first importance to evaluate the IL composition in samples in-pile irradiated at high temperature. Indeed it evidences the predominant influence of the "temperature" parameter on the IL composition.

This work will be further investigated and completed using X-ray tomography methods [18,21].

References

[1] M. K. Meyer, G. L. Hofman, S. L. Hayes, C. R. Clark, T. C. Wiencek, R. V. Strain, & K.-H. Kim, J. Nucl. Mater. 304 (2002), 221-236.

[2] F. Huet, J. Noirot, V. Marelle, S. Dubois, P. Boulcourt, P. Sacristan, S. Naury and P. Lemoine, in: Proceedings of the 9th International Meeting on Research Reactor Fuel Management (RRFM), Budapest (Hungary) 2005, 88-93.

[3] A. Leenaers, S. Van den Berghe, E. Koonen, C. Jarousse, F. Huet, M. Trotabas, M. Boyard, S. Guillot, L. Sannen, and M. Verwerft, J. Nucl. Mater. 335 (2004), 39–47.

[4] S. Van den Berghe, W. Van Renterghem and A. Leenaers, J. Nucl. Mater. 375 (2008), 340-346.

[5] K. Conlon and D. Sears, in: Proceedings of the 10th International Meeting on Research Reactor Fuel Management (RRFM), Sofia (Bulgaria) 2006, 104-108.

[6] K. Conlon and D. Sears, in: Proceedings of the 11th International Meeting on Research Reactor Fuel Management (RRFM), Lyon (France) 2007, 140-144.

[7] O.A. Golosov, V.B. Semerikov et al., in: Proceedings of the 11th International Meeting on Research Reactor Fuel Management (RRFM), Lyon (France) 2007.

[8] J.-S. Lee, C.H. Lee, K. H. Kim, V. Em, J. Nucl. Mater. 306 (2002), 147-152.

[9] H. Palancher, P. Martin, V. Nassif, R. Tucoulou, O. Proux, J.-L. Hazemann, O. Tougait, E. Lahéra, F. Mazaudier, C. Valot and S. Dubois, J. Appl. Crystallogr. 40 (2007), 1065-1075.

[10] H. J. Ryu, Y.S. Han, J.M. Park, S.D. Park and C.K. Kim, J. Nucl. Mater. 321 (2003), 210-220.

[11] F. Mazaudier, C. Proye, F. Hodaj, J. Nucl. Mater. 377 (2008), 476-485.

[12] H. J. Ryu, Y. S. Kim, G.L. Hofman and D.D. Keiser, 28th International Meeting on Reduced Enrichment for Research and Test Reactors (RERTR), Cape Town (south-Africa), 2006.

[13] J. Rodriguez-Carvajal, (1990). FullProf, version 3.40, LLB, CEA/Saclay, France. (http://www.ill.eu/sites/fullprof)

[14] H. Hammersley, (1999). www.esrf.fr/computing/scientific/fit2d

[15] H. Noel, O. Tougait, personal communication (2008).

[16] S.P. Cark, J.R. Ackermann, J. Nucl. Mater. 64 (1977), 265-274.

[17] J.S. Lee, C.H. Lee, K. H. Kim, V. Em, J. Nucl. Mater. 280 (2000), 116-119.

[18] P. Bleuet, E. Welcomme, E. Dooryhee, J. Susini, J.-L. Hodeau, P. Walter, Nature Materials 7 (2008), 468-472.

[19] D.D. Keiser, Argonne National Laboratory Report, ANL-05/14, July (2005).

[20] M. Mirandou, S. Balart, M. Ortiz, S.N. Granovsky, J. Nucl. Mater. 323 (2003), 29-35.

[21] H. Palancher, E. Welcomme, P. Martin, C. Valot, P. Bleuet, R. Tucoulou and P. Lemoine, poster session, this conference.